Small-molecule activators of a bacterial signaling pathway inhibit virulence

Kathryn E. Mansour[1], Yunchuan Qi[2], Mingdi Yan[2], Olof Ramström[2,3], Gregory P. Priebe[1,4], Matthew M. Schaefers[1,4*]

Affiliations:

[1] Division of Critical Care Medicine, Department of Anesthesiology, Critical Care and Pain Medicine, Boston Children's Hospital; Boston, MA, USA

[2] Department of Chemistry, University of Massachusetts Lowell, One University Ave., Lowell, MA 01854

[3] Department of Chemistry and Biomedical Sciences, Linnaeus University, SE-39182 Kalmar, Sweden

[4]Department of Anaesthesia, Harvard Medical School; Boston, MA, USA

*To whom correspondence should be addressed:

Matthew M. Schaefers: Matthew.Schaefers@childrens.harvard.edu 617-919-6133

Keywords: *Burkholderia,* drug-discovery, anti-virulence, two-component systems

Abstract

The *Burkholderia* genus encompasses multiple human pathogens, including potential bioterrorism agents, that are often extensively antibiotic resistant. The FixLJ pathway in *Burkholderia* is a two-component system that regulates virulence. Previous work showed that *fixLJ* mutations arising during chronic infection confer increased virulence while decreasing the activity of the FixLJ pathway. We hypothesized that small-molecule activators of the FixLJ pathway could serve as anti-virulence therapies. Here, we developed a high-throughput assay that screened over 28,000 compounds and identified 11 that could specifically active the FixLJ pathway. Eight of these compounds, denoted *Burkholderia* Fix Activator (BFA) 1-8, inhibited the intracellular survival of *Burkholderia* in THP-1-dervived macrophages in a *fixLJ*-dependent manner without significant toxicity. One of the compounds, BFA1, inhibited the intracellular survival in macrophages of multiple *Burkholderia* species. Predictive modeling of the interaction of BFA1 with *Burkholderia* FixL suggests that BFA1 binds to the putative ATP/ADP binding pocket in the kinase domain, indicating a potential mechanism for pathway activation. These results indicate that small-molecule FixLJ pathway activators are promising anti-virulence agents for *Burkholderia* and define a new paradigm for antibacterial therapeutic discovery.

Introduction

Members of the *Burkholderia* genus can cause serious, difficult to treat infections. Among *Burkholderia* species that cause serious infections in humans are the *Burkholderia cepacia* complex (BCC) and *Burkholderia pseudomallei*. The BCC is composed of approximately 20 species, many of which are significant pathogens for people with cystic fibrosis (CF) and chronic granulomatous disease (CGD)(1-3) and to an ever-growing group of hospitalized patients exposed to contaminated medications or medical devices.(4-17) *B. pseudomallei* causes melioidosis, a serious systemic infection that can include sepsis,

pneumonia, fever, and abscesses. Melioidosis is life-threatening, and mortality can be as high is 50%.(18) *B. pseudomallei* is a potential bioterrorism agent and is classified as a Tier 1 agent by the U.S. Centers for Disease Control and Prevention. Although most commonly found in tropical and sub-tropical soil in South-East Asia and Australia, climate change is thought to have led to the recent isolation of *B. pseudomallei* from soil in Mississippi and Texas, and infections were linked to exposure to this soil.(19-21) *B. pseudomallei* also recently caused a cluster of 4 cases of melioidosis in the U.S. associated with contaminated aromatherapy spray.(22)

Burkholderia are intrinsically resistant to multiple antibiotic classes.(23) This resistance is mediated through alteration of antibiotic targets, decreased outer membrane permeability by modifications of LPS, decreased expression of porins, increased expression of antibiotic-inactivating enzymes, or increased production of efflux pumps.(23, 24) In a study of over 2,000 BCC isolates, more than 50% of the isolates were resistant to chloramphenicol, co-trimoxazole, ciprofloxacin, tetracycline, rifampin, and amoxicillin-clavulanate.(25) One study of 56 CF isolates of *B. dolosa* (a BCC member) found them to be nearly pan-resistant, with minocycline being the only active antibiotic (in just 29% of isolates).(26) Pan-resistance in outbreak strains of *B. cenocepacia* has also been reported.(27) While *B. pseudomallei* isolates are typically susceptible to β-lactam antibiotics, these antibiotics are often not effective at clearing the infection, and treatment can last for months.(18) Thus, novel compounds are needed for *Burkholderia* infections since the number of new prospects from traditional drug development is limited.

Our previous work focused on understanding the role of the *Burkholderia* FixLJ two-component system in pathogenicity. Two-component systems are one mechanism that bacteria use to sense and respond to their environment by modulating gene expression.(28, 29) We initially identified the *Burkholderia fixLJ* two-component system in bacterial whole-genome sequencing studies as being under strong positive selection during chronic *B. dolosa* or *B. multivorans* infection in people with CF.(30-32) The *fixLJ* system regulates ~11% of the genome

of *B. dolosa*(33) and is required for virulence. Our recent work showed that otherwise isogenic BCC constructs carrying evolved (late) *fixL* sequence variants are more virulent than constructs carrying ancestral (early) *fixL* sequence variants.(34) Interestingly, bacteria carrying these evolved *fixL* sequence variants have lower levels of FixLJ pathway activity, demonstrating that high levels of FixLJ pathway activity are detrimental to virulence.(34) These findings led us to the hypothesis that small-molecule activators of the *Burkholderia* FixLJ pathway could make the bacteria less virulent. In the current study, we describe a high-throughput screen that identified 11 novel activators of the *Burkholderia* FixLJ pathway. Eight of these compounds inhibited the virulence of *Burkholderia* in vitro in a *fixLJ*-dependent manner in intracellular survival assays using a macrophage cell line. The most active compound inhibited the virulence of multiple *Burkholderia* species, including *B. thailandensis*, a model organism for *B. pseudomallei*.

Results

High-Throughput Screen Identifies 84 Compounds that Activate the Burkholderia FixLJ Pathway

We developed and conducted a high-throughput screen to look for activators of the *Burkholderia* FixLJ pathway with the goal of identifying novel anti-virulence compounds. We modified an existing *fix* pathway reporter (33, 34) to express green fluorescent protein (GFP) instead of LacZ when the *fixK* promoter is activated by FixLJ. This construct was cloned into a mini-Tn7 based vector allowing for stable integration of the reporter into the *Burkholderia* chromosome without antibiotic selection.(35, 36) This reporter was then conjugated into the clinical CF isolate *B. multivorans* strain VC7102. For the screen, this reporter strain was incubated in 384-well plates in the presence of compounds or DMSO vehicle control, and both OD600 and GFP fluorescence were measured after overnight growth at 37°C (**Figure 1A**). In initial screens we evaluated a library of 640 FDA-approved compounds for their ability to induce the FixLJ pathway. Among this library were several antibiotics and other compounds that

inhibited bacterial growth and GFP activity (lower left region of **Figure S1A**). We identified one compound, an anti-Parkinson's disease drug called benserazide, that was able to induce GFP levels above vehicle (DMSO) treated wells (**Figure S1A**). We sought to confirm benserazide as a hit across two BCC species, and determine if it was *fixLJ*-specific, by using the same GFP reporter conjugated in *B. dolosa* strain AU0158 and its *fixLJ* deletion mutant. If benserazide specifically targeted FixLJ, there would not be an increase in fluorescence seen in the *fixLJ* deletion mutant when treated with benserazide. Benserazide was able to induce GFP response in a dose-dependent manner in both *B. multivorans* and *B. dolosa* (**Figure S1B**), but was it also induced a GFP response in the *fixLJ* deletion mutant, demonstrating that benserazide activates the GFP reporter in a *fixLJ* independent mechanism. Benserazide was subsequently used a positive fluorescence control in screening assays.

Next, 28,100 compounds were screened, with each assay plate including at least 1 column (16 wells) that contained DMSO (vehicle) alone as a negative control and at least 1 column (16 wells) that contained benserazide which served as a positive fluorescence control (**Figure 1**). Using benserazide as a positive fluorescence control and DMSO as a negative control, we were able to achieve Z' factors ~0.5, indicating the screening assay was technically robust.(37) We identified an additional 83 hits having mean fluorescence of the 2 replicate plates at least 3 standard deviations above the plate-specific negative control. Compounds were identified as weak hits if their increase in fluorescence was between 3-6 standard deviations above the negative control mean. Moderate hits had an increase in fluorescence between 6-9 standard deviations, and strong hits were at least 9 standard deviations above the mean negative control value (**Table 1**). These 83 compounds were "cherry-picked" from compound library plates, and their ability to induce GFP activity in *B. dolosa* strain AU0158 and its *fixLJ* deletion mutant was assessed to confirm FixLJ-specific activation of the GFP reporter (**Table S1**). We found that most compounds activated the GFP reporter to similar levels in the parental *B. dolosa* strain as in the *fixLJ* deletion mutant, indicating that these compounds were activating

the reporter in a FixLJ-independent manner. We did find 7 compounds that activated the GFP reporter only in the parental *B. dolosa* strain, and we therefore classified these as type 1 hits (Red dots, **Figure 1C**). We also identified 4 compounds that were classified as hits in both the parental *B. dolosa* strain and the *fixLJ* deletion mutant, but were a lesser strength hit in the *fixLJ* deletion mutant compared the parental *B. dolosa*, so these were classified as type 2 hits (Blue dots, **Figure 1C**). It is important to note that these hits did not inhibit bacterial growth in the screen. In total we identified 11 compounds that were able to activate the FixLJ pathway (either type 1 or 2 hits), 10 of which were available commercially. The structures of these 10 compounds are depicted in **Figure 1,** and full chemical names are listed in Table S2.

Table 1. Number of hits from primary screen and number of hits confirmed to be *fixLJ*-specific.

Type of Hit	# of Hits in Primary Screen	# of Confirmed *fixLJ*- Specific Hits
Strong	15	3
Medium	11	4
Weak	57	4

Eight of the Small-molecule FixLJ Activators Inhibit Burkholderia Virulence in vitro

We tested the ability of the 10 hits to inhibit *B. dolosa* invasion of and/or intracellular survival within macrophages, which is a critical aspect of *Burkholderia* virulence.(38-40) Here, we used *B. dolosa* strain AU0158, a CF clinical isolate that also employed in the screen. In these assays, THP-1 cells are differentiated into macrophage-like cells using phorbol 12-myristate-13-acetate (PMA) and infected with *Burkholderia* (5-10 bacteria per macrophage) for two hours while being exposed to compound or vehicle (DMSO). Cells were washed and then treated with kanamycin (to kill extracellular bacteria) along with compound or DMSO for an additional 2-4 hours. Cells were washed again, lysed, and then colony forming units (CFU) were determined by serial dilution and plating (**Figure 2A**). Eight of the 10 compounds inhibited invasion/survival of *B. dolosa* in macrophages and were named *Burkholderia* Fix Activator

(BFA) 1-8 (**Figure 2**). BFA1 inhibited *B. dolosa* virulence at concentrations as low as the lowest tested dose of 1.5 μM (**Figure 2B**) while the other 7 compounds inhibited virulence at concentrations between 6.25 and 12.5 μM (**Figure 2C-I**). BFA compounds 2-8 inhibited the invasion/survival of *B. dolosa* up to 50% at the highest dose of compound tested. BFA1 was able to inhibit invasion/survival of *B. dolosa* in macrophages by ~75%. This reduction in the number of intracellular bacteria was *fixLJ*-specific, as the *B. dolosa fixLJ* deletion mutant, which already is less virulent than its parental strain as previously reported,(33) did not have significant reductions in intracellular bacteria when treated with any of the BFA compounds (**Figure 2,** red bars). Two of the 10 hits were not able to inhibit the invasion/survival of *B. dolosa* in macrophages (**Figure 2J and 2K**) and were not further evaluated.

We also measured the cytotoxicity of BFA compounds by measuring lactate dehydrogenase (LDH) release from a human lung epithelial cell line (A549) and from THP-1 derived macrophages using commercially available kits. As shown in **Figure S2**, we found that none of the compounds caused significant cytotoxicity after overnight exposure at any of the tested concentrations. These findings demonstrate that BFA compounds can inhibit the virulence of *Burkholderia* in a *fixLJ*-specific mechanism without significant toxicity *in vitro*.

In additional to measuring the ability of BFA compounds to inhibit the virulence of *B. dolosa*, we measured the ability of select BFA compounds to inhibit the invasion of and/or intracellular survival of other pathogenic *Burkholderia* species using the same THP-1-dervied macrophage infection model. We measured the ability of 7 of the 8 BFA compounds (25 μM) to inhibit invasion/intracellular survival of *B. cenocepacia, B. multivorans,* and *B. thailandensis*. *B. thailandensis* is a model for *B. pseudomallei* that does not require BSL3 facilities.(41) We were unable to obtain sufficient amounts of BFA4 for further analysis, so it was excluded. BFA1 inhibited the invasion/survival of all three additional *Burkholderia* species (**Figure 3A-3C**). All seven of the tested BFA compounds inhibited the invasion/survival of *B. multivorans* (**Figure 3A**). BFA1 was also able to inhibit the invasion/survival of *B. cenocepacia* (**Figure 3B**) and *B.*

thailandensis (**Figure 3C**). BFA6 was also able to inhibit the invasion/survival of *B. thailandensis* (**Figure 3C**), while there was a trend towards significance for other BFA compounds to inhibit *B. thailandensis*. Since BFA1 had the highest activity, multiple doses were evaluated for their ability to inhibit invasion/survival of other *Burkholderia.* Doses of 6.25 μM of BFA1 inhibited the invasion/survival of *B. multivorans* (**Figure 3D**) and *B. thailandensis* (**Figure 3F**), while higher doses were needed to inhibit *B. cenocepacia* (**Figure 3E**).

In silico Docking Studies Demonstrate BFA1 Interaction with ATP/ADP-Binding Pocket of FixL

We performed docking studies with *B. dolosa* FixL (AlphaFold ID: A0A0D5J096) using AutoDockFR in the flexible residue mode.[42] Initial AutoSite calculations predicted two major potential ligand-binding sites on the protein (**Figure S3A**, **Table 2**), of which the site with the highest affinity strongly resembled the ATP/ADP binding site of known histidine kinases, such as the structures from *Caulobacter vibrioides* (PDB ID: 5IDJ),(43) *Lactiplantibacillus plantarum* (4ZKI),(44) or *Thermotoga maritima* (6RH8).[45] This site was thus chosen as the primary docking target, to which docking with ADP yielded a binding interaction similar to the mentioned histidine kinases, thereby validating the docking process (**Figure S3B**).

Table 2. Potential ligand-binding pocket parameters.

Pocket	AutoSite score	Number of points	Radius of gyration	Buriedness
1	43.69	347	5.71	0.85
2	39.25	301	5.18	0.82

As expected, the predicted score for ADP binding to the second pocket was considerably lower. On the other hand, the binding scores for compound BFA1 were of similar magnitude for the two sites, in both cases better than for ADP (**Table S3**). For the ATP/ADP binding site, the docking analysis showed interactions between compound BFA1 and several

203 residues in the binding pocket, with the coumarin oxygen atoms interacting with Gly777,
204 Leu778, Thr769, and the oxadiazole oxygen interacting with Met776 (**Figure 4A, Figure S3C**).
205 For the secondary binding site, the analysis revealed polar interactions between the ligand and
206 residues Arg585, Asn779, and Ser783, as well as more lipophilic interactions with nonpolar
207 residues (**Figure S3D**). Docking simulations were also carried out using HADDOCK 2.4,(46, 47)
208 revealing similar binding trends (**Tables S3 and S4**). A potential effect may also arise from
209 binding to the second pocket, although the results in this case indicate a lower degree of more
210 specific polar interactions compared to the ADP/ATP binding site.
211
212 **Discussion**
213 In this study we developed a high-throughput screen to identify small molecules that
214 activate the *Burkholderia* FixLJ pathway, with the goal of inhibiting the virulence of these
215 pathogens. This approach was based on our previous work that found mutations within the *fixL*
216 gene leading to lower FixLJ pathway activity were selected for during chronic infection in people
217 with CF(30, 31) and correlated with periods of decline in lung function in people with CF.(34)
218 These findings lead us to the hypothesis that a small molecule activating the FixLJ pathway
219 could make *Burkholderia* less pathogenic, in a way coaxing the bacteria back to its soil
220 existence where FixLJ activity is high.
221 Our high-throughput screen identified 8 compounds we call Burkholderia Fix Activators
222 (BFA). These compounds previously had no known biological activity. All 8 of the BFA
223 compounds inhibited the invasion and/or intracellular survival of *B. dolosa* in a *fixLJ*-specific
224 manner (**Figure 2**) but had no impact on bacterial growth in rich media. BFA1 inhibited virulence
225 at a lower concentration and at a greater magnitude than the other BFA compounds. The BFA
226 compounds caused no significant cytotoxicity, measured by LDH release, after 24-hour
227 incubation suggesting macrophage death plays a negligible role in the BFA activity in antibiotic
228 exclusion assays. *Burkholderia* are known for their extensive antibiotic resistance that is often

mediated by decreases in outer membrane permeability and increases in efflux pump activity.(23, 24) Since clinical isolates of *Burkholderia* were used in our assays that identified the BFA compounds, it is clear that the BFA compounds are able to overcome these intrinsic drug penetration obstacles that have hindered antibiotic development.

The *in silico* predicted binding of BFA 1 to the ATP/ADP binding pocket of FixL with a higher affinity than ADP is, on first review, counterintuitive for a molecule that increases FixL activity. However, for rhizobial FixL, ADP binding has been shown to decrease the affinity of FixL for oxygen, which results in activation of FixL.(48) This activation is related to the homodimer properties of FixL(49) whereby ADP that is formed as part of the autophosphorylation of FixL binds to FixL, which decreases the binding affinity to oxygen in the other FixL molecule of the homodimer. This, in turn, allows for a positive feedback resulting in increased FixL activation.(48) Thus, BFA1 binding to FixL at this same pocket is predicted to increase FixL activation as a result of decreased binding affinity for oxygen. These predictions are supported by findings that single amino acid changes of the asparagine residue (403) in the ADP-binding site of rhizobial FixL resulted in no change in oxygen affinity in response to ADP binding, demonstrating the importance of this residue in ADP binding.(48) The homologous asparagine in the predicted ADP-binding site of *Burkholderia* FixL is at amino acid 715 and is predicted to interact with or be adjacent to BFA1 or ADP binding (**Figure 4** and **S3**). The predicted mechanism of action is depicted in **Figure 4F**, where BFA1 binds to FixL via the ATP/ADP binding pocket on the protein, which causes a decrease in binding affinity to oxygen and, in turn, activates FixL. FixL autophosphorylates, then transfers the phosphate group to the response regulator FixJ. Phosphorylated FixJ then binds to DNA and turns on transcription of target genes that are part of the FixLJ regulon resulting in a gene expression profile making the bacteria less virulent.

Our method of using small-molecule activators of a pathway to inhibit the virulence of antibiotic-resistant pathogens is a novel approach for the development of new antibacterial

255 therapies. Most of the other limited number of studies investigating two-component systems as
256 drug targets have focused on two-component systems that are involved in quorum sensing
257 pathways and other pathways required for bacterial growth.(28, 50-53) Other groups have
258 identified compounds that inhibit bacterial two-component systems to make pathogens less
259 virulent,(54-59) highlighting that two-component systems can be targeted in multiple ways to
260 make a pathogen less virulent. By targeting bacterial virulence rather than bacterial growth, the
261 emergence of resistance to therapies will be slower to occur.(60) We expect that resistance to
262 our lead compound, BFA1, will be slow to develop since the amino acids of FixL predicted to be
263 involved in binding to BFA1 are outside the FixL domains where mutations are seen during
264 chronic infection.(30, 31) In conclusion, our results show that small-molecule activators of the
265 *Burkholderia* FixLJ pathway are a promising new anti-virulence approach.
266
267

Methods

Bacterial strains, plasmids, cell lines, and growth conditions

Bacterial strains used and generated in this study are listed in **Table 3**. For the generation of the reporter strain, BCC and *E. coli* were grown on LB plates or in LB medium and supplemented with following additives: ampicillin (100 µg/mL), chloramphenicol (20 µg/mL), trimethoprim (100 µg/mL for *E. coli,* 1 mg/mL for BCC), gentamicin (50 µg/mL). For some experiments, trypticase soy broth (TSB) or trypticase soy agar (TSA) was used for growth of *Burkholderia*. Human monocyte line THP-1 and human lung epithelial cell line A549 were obtained from ATCC and grown at 37°C with 5% CO_2. THP-1 cells were cultured in RPMI-1640 medium containing 2 mM L-glutamine, 10 mM HEPES, 1 mM sodium pyruvate, 4500 mg/L glucose, and 1500 mg/L sodium bicarbonate, supplemented with 10% heat-inactivated fetal calf serum (FCS, Gibco) and 0.05 mM 2-mercaptoethanol. A459 cells were grown in RPMI 1640 with L-glutamine and 10% heat-inactivated fetal calf serum (FCS, Gibco). Penicillin and streptomycin were added for routine culture but were removed the day before and during experiments.

Table 3. Strains used in this study.

	Notes	Source
E.coli		
NEB 5-alpha Competent *E. coli*	DH5α derivative cloning strain	NEB
Burkholderia		
B. dolosa AU0158	Clinical isolate	John LiPuma
B. dolosa AU0158 Δ*fixLJ*	Clean, unmarked *fixLJ* deletion mutant	(33)
B. multivorans VC7102	Clinical isolate	(32)

B. multivorans VC7102 Fix-GFP Reporter	*B. multivorans* VC7102 + Fix-GFP reporter	This study
B. dolosa AU0158 Fix-GFP Reporter	*B. dolosa* AU0158 + Fix-GFP reporter integrated at *att*Tn7 site downstream of AK34_4894	This study
B. dolosa AU0158 Δ*fixLJ* Fix-GFP Reporter	*B. dolosa* Δ*fixLJ* + Fix-GFP reporter integrated at *att*Tn7 site downstream of AK34_4894	This study
B. thailandensis strain e264	Isolate from rice field in Thailand, model for *Burkholderia pseudomallei*	ATCC
B. cenocepacia K56-2	Clinical Isolate	Joanna Goldberg

284
285

286 ***Genetic Manipulations and Strain Construction***

287 All plasmids used and generated in this study are listed in **Table 4**. To generate the GFP
288 reporter of FixLJ pathway activity (Fix-GFP reporter), we cloned the first 23 bp of *fixK* and the
289 immediate 243 bp upstream of the start codon from pfixK-reporter(33) in-frame with eGFP gene
290 from pIN301 into the multiple cloning site of pUC18-mini-Tn7-Tp. Use of a mini-Tn7 vector
291 allows for stable chromosomally integration at an *att*Tn7 site.(36, 61) The plasmid was
292 transformed into NEB 5-alpha competent *E. coli,* and the sequence of the plasmid was
293 confirmed using PCR and Sanger sequencing. The Fix-GFP reporter was conjugated into *B.*
294 *dolosa* strain AU0158, the AU0158 *fixLJ* deletion mutant, and *B. multivorans* strain VC7102 with
295 pRK2013 and pTNS3 using published procedures.(33) Conjugants were selected for by plating
296 on LB agar containing trimethoprim (1 mg/mL) and gentamicin (50 µg/mL). Insertions into the

297 *att*Tn7 site downstream of AK34_4894 was confirmed by PCR of *B. dolosa* strains as previously
298 published.(33, 34)

299 **Table 4.** Plasmids used in this study.

	Notes	Source
pTNS3	Amp^R, helper plasmid for mini-Tn7 integration into *att*Tn7 site	(35)
pRK2013	Km^R conjugation helper	(61)
pUC18T-mini-Tn*7*T-Tp	Amp^R, Tp^R on mini-Tn*7*T; mobilizable	(61)
pfixK-reporter	pSCrhaB2 carrying *B. dolosa fixK* promoter -*lacZ* fusion,Tp^R	(33)
pIN301	eGFP, CmR	Annette Vergunst
Fix-GFP reporter	*fixK* promoter -GFP fusion in pUC18T-mini-Tn*7*T-Tp	This study

300
301

302 ***Small Molecule High Throughput Screens***

303 Small-molecule screens were conducted at Institute of Chemistry and Cell Biology (ICCB) -
304 Longwood Screening Facility at Harvard Medical School. *B. multivorans* strain VC7102, with
305 Fix-GFP reporter, was grown overnight in TSB at 37°C with shaking and diluted 1:100 in fresh
306 TSB the day of the assay. 30 µL per well was added into a black clear-bottom 384-well plate
307 using Thermo Multidrop Combi pipette. 30 µL per well of TSB was also added into each well
308 containing a test compound using the Combi pipette. Wells that served as negative controls

contained 30 µL of TSB plus DMSO (0.078% v/v in TSB, final concentration 0.039%). For positive fluorescence control wells, we added 30 µL of TSB containing 78 µM of benserazide (final concentration 39 µM). 300 nL solutions of each compound in DMSO were pin-transferred to each plate using an Epson Compound Transfer Robot from a compound library plate. For most compound library plates the stock concentration was 10 nM, but some plates had different concentrations typically 1-10 mM, details are posted in screen data deposited in PubChem. For every assay, 2 replicate assay plates were set up. Initial OD600 and GFP fluorescence were measured using PerkinElmer EnVision with Photometric 600 filter (600 nm, 8 nm bandpass), FITC 535 (Excitation filter FITC 585, Emission Filter FITC 535). Plates were stacked 5 high, covered with lids, and incubated at 37 °C overnight (~18 h). The following day, assay plates were read using the PerkinElmer EnVision as above. For each well, the initial GFP fluorescence intensity values were subtracted from overnight GFP fluorescence intensity values to calculate the ΔGFP for each well. The average ΔGFP was calculated by averaging the 2 replicate wells for each library well. The mean and standard deviation for ΔGFP of the negative control wells on the replicate plates was calculated. A compound was determined to be a strong hit if the average ΔGFP was more than 9 standard deviations above mean ΔGFP for the negative control wells on the 2 replicate plates. A compound was determined to be a moderate hit if the average ΔGFP was more than 6 standard deviations above mean ΔGFP for the negative control, and a compound was determined to be a weak hit if the average ΔGFP was more than 3 standard deviations above mean ΔGFP for the negative control for its respective plate. Subsequent analysis of data from the primary screen identified 3 additional hits that were not identified in first analysis and were not further evaluated. For “cherry-pick” studies, overnight cultures of *B. multivorans* strain VC7102*, B. dolosa* strain AU0158, and *B. dolosa* strain AU0158 *fixLJ* deletion mutant were diluted and plated in wells of a 384-well plate. 300 nL of selected compounds were plated into wells using a HP D300e liquid dispenser so that 2 wells of each bacterial strain were

334 treated with compound. Plates were incubated, and the OD600 and GFP fluorescence intensity
335 were measured as described above.
336
337 ***Bacterial invasion assays***
338 The ability of BFA compounds to inhibit the uptake of and/or intracellular survival of
339 *Burkholderia* into THP-1-dervived macrophages was determined using published protocols.(33,
340 34) Human THP-1 monocytes were differentiated into macrophages by seeding 1 mL into 24-
341 well plates at $7.5x10^5$ cells/mL with 200 nM phorbol 12-myristate 13-acetate (PMA). Log-phase
342 *Burkholderia* were grown and washed in RPMI containing 10% heat-inactivated FCS three times
343 and diluted to ~$2x10^6$ CFU/mL and mixed with BFA compounds or DMSO (vehicle control). 1
344 mL/ well (MOI of ~10:1) of the bacterial suspension was used to infect THP-1 derived
345 macrophages. Plates were spun at 500 g for 5 minutes to synchronize infection and then
346 incubated for 2 hours at 37°C with 5% CO_2. To determine the number of intracellular bacteria,
347 separate infected wells were washed two times with PBS and then incubated with RPMI plus
348 10% heat-inactivated FCS containing BFA or DMSO (vehicle control) with kanamycin (1 mg/mL)
349 or kanamycin plus ceftazidime (1 mg/mL each for *B. cenocepacia*) for 2-4 hours. Monolayers
350 were washed three times with PBS, lysed with 1% Triton-X100, serially diluted, and plated to
351 enumerate the number of bacteria.
352
353 ***LDH release assay***
354 A549 cells were grown to confluence in 96-well plates. Human THP-1 monocytes were
355 differentiated into macrophages by 72-hour PMA treatment and seeded into 96-well plates at
356 density of $7.5x10^4$ cells/well. A549 cells and THP-1-deried macrophages were then treated with
357 BFA (0-25 μM in DMSO) for 24 hours. LDH release was measured within supernatants using
358 CytoTox 96® Non-Radioactive Cytotoxicity Assay (Promega) per manufacture's protocol. For a
359 positive control, untreated wells were incubated with 10X lysis buffer (provided with kit) during

the last 30 minutes. Percent cytotoxicity was determined relative to maximum LDH release from cells treated with lysis buffer.

In silico docking studies

Docking studies were performed using AutoDockFR Suite 1.0 in the flexible residue mode.[42] Calculations were performed with 8 independent searches, each of which with 50 genetic algorithm evolutions associated with 2×10^6 evaluations of the scoring function. Potential binding sites were identified by AutoSite 1.0. Residues Asn715, Tyr767, Ser768, Thr769, and Lys770 were set as flexible for pocket 1 and residues Arg585, Asn779, Ser783 for pocket 2. Docking simulations were also carried out using HADDOCK 2.4,(46, 47) using the default settings for small molecule-protein docking with RMSD-based clustering. The regions of the two binding sites identified by ADFR were investigated using corresponding active residues (Asn715, Tyr767, Ser768, Thr769, Lys770 at pocket 1; Arg585, Asn779, Ser783 at pocket 2). 1000 structures were generated initially and 200 clusters were screened out after refinement. All docking results were visualized by UCSF Chimera 1.17.3 and LigPlot+ 2.2.(62, 63)

Data Availability

Data from the high-throughput screen are deposited to PubChem AID 1918990.

Acknowledgements

We would like to thank the staff of the Institute of Chemistry and Cell Biology (ICCB) - Longwood Screening Facility at Harvard Medical School for their assistance with the screening assays. This work was funded by National Institutes of Health (R21AI159211 to MMS), the Department of Anesthesiology, Critical Care and Pain Medicine at Boston Children's Hospital (Trailblazer Award and Transition to Independence Award to MMS, no numbers), and the Cystic

Fibrosis Foundation (PRIEBE13I0 to GPP). OR and MY thank the University of Massachusetts Lowell for financial support (No Number).

Author Contributions

GPP and MMS conceived of the idea for the study. KEM, YQ, MY, OR and MMS conducted the experiments. MY, OR, GPP and MMS acquired funding. MY, OR, GPP, and MMS supervised. KEM and MMS drafted original draft, all authors revised and approved final version.

393

394 **Figures**

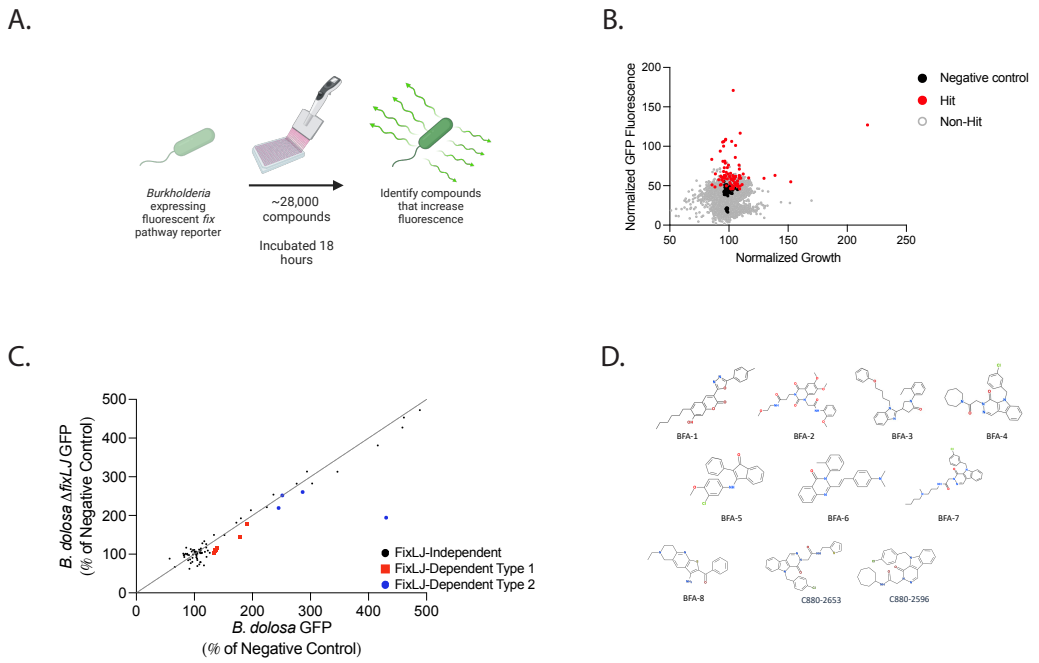

395

396 **Figure 1. A high-throughput screen identifies 84 small molecules that activate the**

397 **Burkholderia FixLJ pathway, 11 of which are *fixLJ*-specific.** (A.) Schematic of the screen.

398 Created with BioRender. (B.) Scatter plot from high-throughput screen of 28,100 compounds for

399 activators of GFP activity in *B. multivorans* strain VC7102 carrying a GFP reporter for FixLJ

400 pathway activity. GFP fluorescence and growth OD600 values are normalized based on plate-

401 specific benserazide treated wells. Dots are averages of two replicate wells treated with same

402 compound. Hits (red dots) have that GFP activity more than 3 standard deviations above the

403 plate-specific mean negative control wells (DMSO, black dots). (C.) Scatter plot of 84 hits from

404 primary screen chosen for follow-up assays measuring the GFP signal in *B. dolosa* and its *fixLJ*

405 deletion mutant to assess dependence on FixLJ pathway. The GFP as percent of negative

406 control (DMSO-treated) for each compound is plotted as GFP seen the *fixLJ* deletion mutant vs.

407 parental strain. Type 1 hits (red) have that GFP activity more than 3 standard deviations above

408 the plate-specific mean negative control wells in the parental strain, but not in the *fixLJ* deletion
409 mutant. Type 2 hits (blue) are categorically greater hits in strength in the parental strain
410 compared to the hit strength in the *fixLJ* deletion mutant. (D.) Structures of the 10 of the 11
411 *fixLJ*-dependent hits. These ten compounds were available from ChemDiv.
412

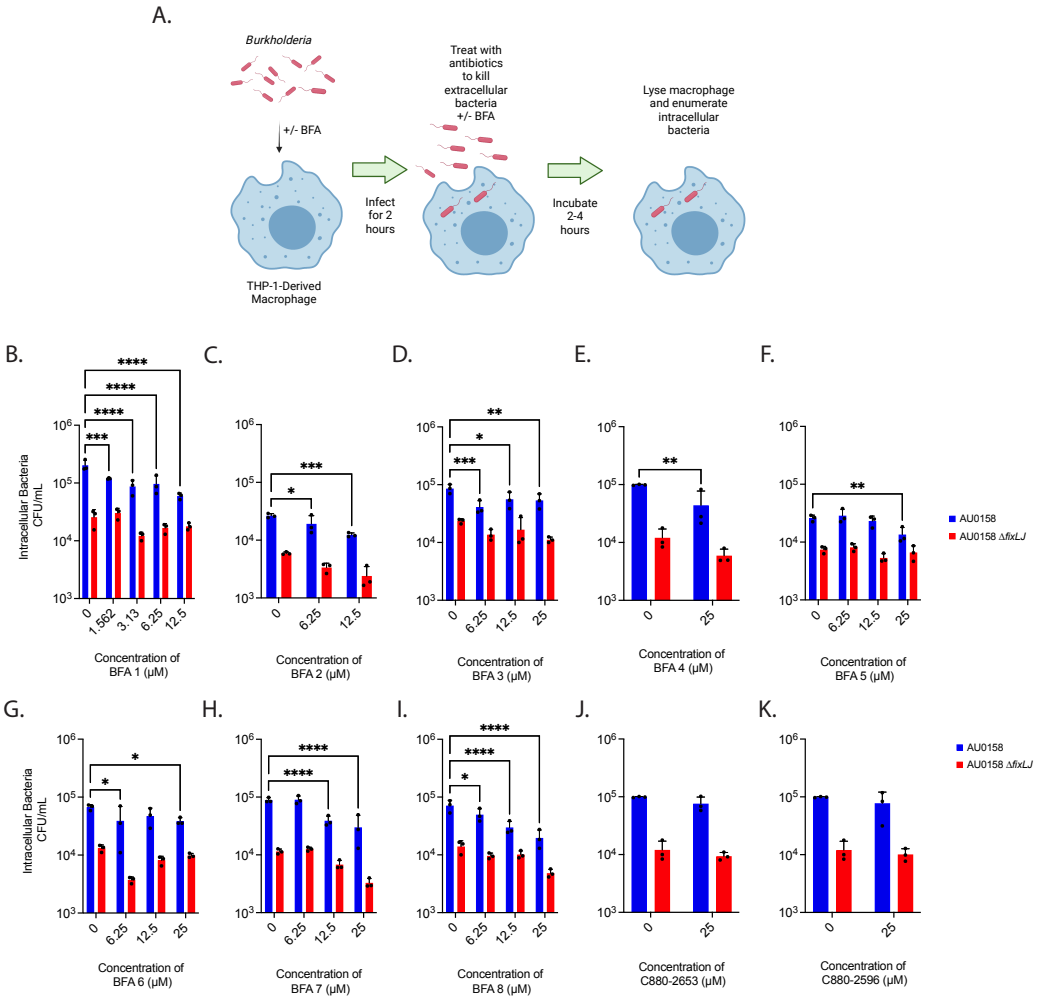

413

414 **Figure 2. BFA (Burkholderia Fix Activator) compounds inhibit *B. dolosa* virulence in THP-**
415 **1-derived macrophages in a *fixLJ*-specific manner.** The intracellular survival (and/or uptake)
416 of *B. dolosa* strain AU0158 in THP-1-derived human macrophages was measured using an
417 antibiotic exclusion assay in the presence of varying concentrations BFA compounds. Created
418 with BioRender. (A). The number of intracellular bacteria was determined by lysing the

419 macrophages and enumerating CFU after incubation for 2 hours (B,D) or 4 hours
420 (C,E,F,F,G,H,I,J,K). *, **, and *** denote p<0.05, 0.01, and 0.001, respectively, by two-way
421 ANOVA with Dunnett's multiple comparisons test using 0 μM (DMSO vehicle) as control.
422

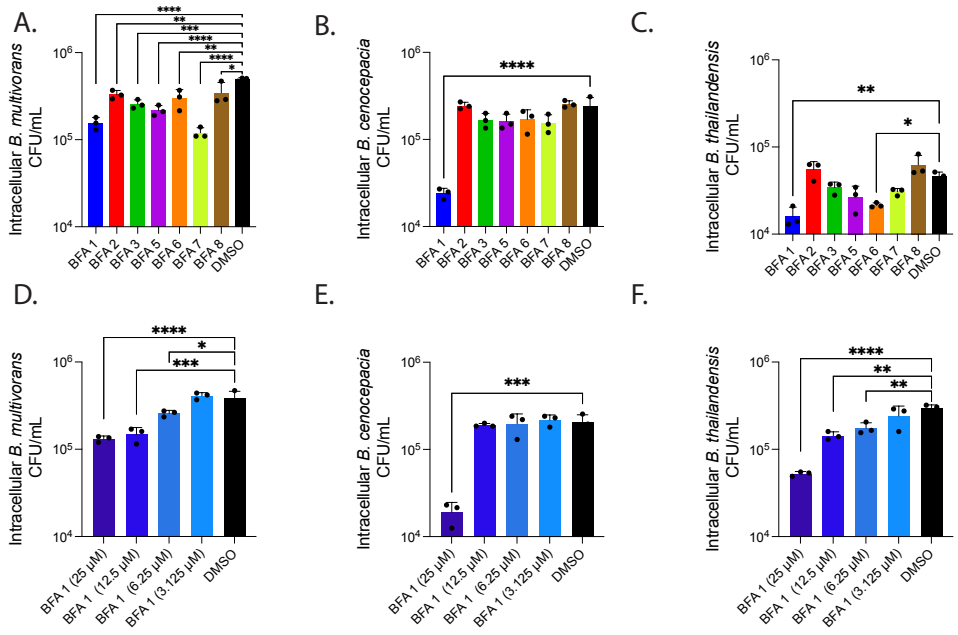

423

424 **Figure 3. BFA compounds inhibit the virulence of multiple pathogenic *Burkholderia***
425 ***species.*** THP-1-derived macrophages were infected with *B. multivorans* strain VC7102 (A&D),
426 *B. cenocepacia* strain K56-2 (B&E), or *B. thailandensis* strain e264 (C&F) in the presence of 25
427 μM of BFA compounds (A-C) or a dose range of BFA1 (D-F). Intracellular bacteria were
428 determined using antibiotic exclusion after 2 (F) or 4 (A-E) hour exposure to antibiotic. *P* value
429 determined by ANOVA with Dunnett's multiple comparisons test, *, **,***,**** denotes *p* value <
430 0.05,0.01, 0.001, 0.0001, respectively.
431
432

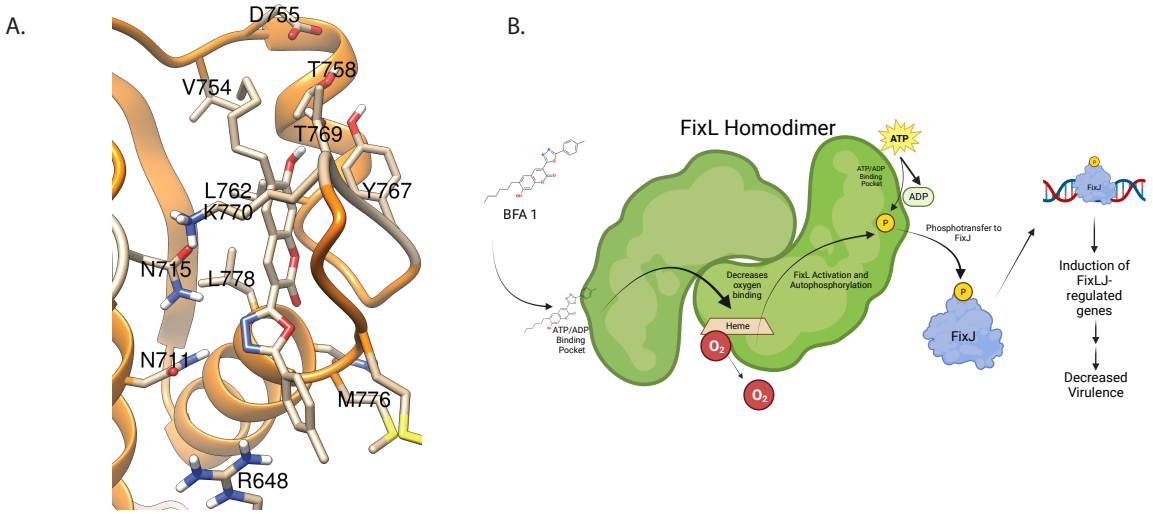

Figure 4. BFA1 is predicted to bind to FixL at the ATP/ADP-binding pocket of the histidine kinase domain. (A) Predicted binding of BFA1 to first binding pocket of *B. dolosa* strain AU0158 FixL using AutoDockFR. (B) Proposed mechanism of action for BFA1 activating *Burkholderia* FixLJ pathway. Created with BioRender.

References

1. Gibson RL, Burns JL, Ramsey BW. Pathophysiology and management of pulmonary infections in cystic fibrosis. Am J Resp Crit Care Med. 2003;168(8):918-51.
2. Lipuma JJ. The changing microbial epidemiology in cystic fibrosis. Clin Microbiol Rev. 2010;23(2):299-323.
3. Marciano BE, Spalding C, Fitzgerald A, Mann D, Brown T, Osgood S, et al. Common severe infections in chronic granulomatous disease. Clin Infect Dis. 2015;60(8):1176-83.
4. Dolan SA, Dowell E, LiPuma JJ, Valdez S, Chan K, James JF. An outbreak of *Burkholderia cepacia* complex associated with intrinsically contaminated nasal spray. Infect Control Hosp Epidemiol. 2011;32(8):804-10.
5. Souza Dias MB, Cavassin LG, Stempliuk V, Xavier LS, Lobo RD, Sampaio JL, et al. Multi-institutional outbreak of *Burkholderia cepacia* complex associated with contaminated mannitol solution prepared in compounding pharmacy. Am J Infect Control. 2013;41(11):1038-42.
6. Vardi A, Sirigou A, Lalayanni C, Kachrimanidou M, Kaloyannidis P, Saloum R, et al. An outbreak of *Burkholderia cepacia* bacteremia in hospitalized hematology patients selectively affecting those with acute myeloid leukemia. Am J Infect Control. 2013;41(4):312-6.

7. Antony B, Cherian EV, Boloor R, Shenoy KV. A sporadic outbreak of *Burkholderia cepacia* complex bacteremia in pediatric intensive care unit of a tertiary care hospital in coastal Karnataka, South India. Indian J Pathol Microbiol. 2016;59(2):197-9.
8. Glowicz J, Crist M, Gould C, Moulton-Meissner H, Noble-Wang J, de Man TJB, et al. A multistate investigation of health care-associated *Burkholderia cepacia* complex infections related to liquid docusate sodium contamination, January-October 2016. Am J Infect Control. 2018.
9. Marquez L, Jones KN, Whaley EM, Koy TH, Revell PA, Taylor RS, et al. An outbreak of *Burkholderia cepacia* complex infections associated with contaminated liquid docusate. Infect Control Hosp Epidemiol. 2017:1-7.
10. Song JE, Kwak YG, Um TH, Cho CR, Kim S, Park IS, et al. Outbreak of *Burkholderia cepacia* pseudobacteraemia caused by intrinsically contaminated commercial 0.5% chlorhexidine solution in neonatal intensive care units. J Hosp Infect. 2018;98(3):295-9.
11. Cunha BA, Gian J, Dieguez B, Santos-Cruz E, Matassa D, Gerson S, et al. *Burkholderia contaminans* Colonization from Contaminated Liquid Docusate (Colace) in a Immunocompetent Adult with Legionnaire's Disease: Infection Control Implications and the Potential Role of *Candida pellucosa*. J Clin Med. 2016;5(12).
12. Deng P, Wang X, Baird SM, Showmaker KC, Smith L, Peterson DG, et al. Comparative genome-wide analysis reveals that *Burkholderia contaminans* MS14 possesses multiple antimicrobial biosynthesis genes but not major genetic loci required for pathogenesis. Microbiologyopen. 2016;5(3):353-69.
13. Martin M, Christiansen B, Caspari G, Hogardt M, von Thomsen AJ, Ott E, et al. Hospital-wide outbreak of *Burkholderia contaminans* caused by prefabricated moist washcloths. J Hosp Infect. 2011;77(3):267-70.
14. Moehring RW, Lewis SS, Isaacs PJ, Schell WA, Thomann WR, Althaus MM, et al. Outbreak of bacteremia due to *Burkholderia contaminans* linked to intravenous fentanyl from an institutional compounding pharmacy. JAMA Intern Med. 2014;174(4):606-12.
15. Nannini EC, Ponessa A, Muratori R, Marchiaro P, Ballerini V, Flynn L, et al. Polyclonal outbreak of bacteremia caused by *Burkholderia cepacia* complex and the presumptive role of ultrasound gel. Braz J Infect Dis. 2015;19(5):543-5.
16. Seelman SL, Bazaco MC, Wellman A, Hardy C, Fatica MK, Huang MJ, et al. *Burkholderia cepacia* complex outbreak linked to a no-rinse cleansing foam product, United States - 2017-2018. Epidemiol Infect. 2022;150:e154.
17. Rhee C, Baker MA, Tucker R, Vaidya V, Holtzman M, Seethala RR, et al. Cluster of *Burkholderia cepacia* Complex Infections Associated With Extracorporeal Membrane Oxygenation Water Heater Devices. Clin Infect Dis. 2022;75(9):1610-7.
18. Wiersinga WJ, Virk HS, Torres AG, Currie BJ, Peacock SJ, Dance DAB, et al. Melioidosis. Nat Rev Dis Primers. 2018;4:17107-.
19. CDC. Melioidosis Locally Endemic in Areas of the Mississippi Gulf Coast after *Burkholderia pseudomallei* Isolated in Soil and Water and Linked to Two Cases – Mississippi, 2020 and 2022 2022 [Available from: https://emergency.cdc.gov/han/2022/han00470.asp.
20. Hall CM, Romero-Alvarez D, Martz M, Santana-Propper E, Versluis L, Jiménez L, et al. Low risk of acquiring melioidosis from the environment in the continental United States. PLOS ONE. 2022;17(7):e0270997.
21. Torres AG. The public health significance of finding autochthonous melioidosis cases in the continental United States. PLOS Neglected Tropical Diseases. 2023;17(8):e0011550.
22. Gee JE, Bower WA, Kunkel A, Petras J, Gettings J, Bye M, et al. Multistate Outbreak of Melioidosis Associated with Imported Aromatherapy Spray. New England Journal of Medicine. 2022;386(9):861-8.
23. Rhodes KA, Schweizer HP. Antibiotic resistance in *Burkholderia* species. Drug Resist Updat. 2016;28:82-90.

24. Podnecky N, Rhodes K, Schweizer H. Efflux Pump-mediated Drug Resistance in *Burkholderia*. Frontiers in Microbiology. 2015;6(305).
25. Zhou J, Chen Y, Tabibi S, Alba L, Garber E, Saiman L. Antimicrobial Susceptibility and Synergy Studies of *Burkholderia cepacia* Complex Isolated from Patients with Cystic Fibrosis. Antimicrob Agents Chemother. 2007;51(3):1085.
26. Skurnik D, Davis MR, Jr., Benedetti D, Moravec KL, Cywes-Bentley C, Roux D, et al. Targeting pan-resistant bacteria with antibodies to a broadly conserved surface polysaccharide expressed during infection. J Infect Dis. 2012;205(11):1709-18.
27. Sass A, Marchbank A, Tullis E, Lipuma JJ, Mahenthiralingam E. Spontaneous and evolutionary changes in the antibiotic resistance of *Burkholderia cenocepacia* observed by global gene expression analysis. BMC Genomics. 2011;12:373.
28. Schaefers MM. Regulation of Virulence by Two-Component Systems in Pathogenic *Burkholderia*. Infection and immunity. 2020;88(7).
29. Capra EJ, Laub MT. Evolution of two-component signal transduction systems. Annual review of microbiology. 2012;66:325-47.
30. Lieberman TD, Flett KB, Yelin I, Martin TR, McAdam AJ, Priebe GP, et al. Genetic variation of a bacterial pathogen within individuals with cystic fibrosis provides a record of selective pressures. Nature genetics. 2014;46(1):82-7.
31. Lieberman TD, Michel JB, Aingaran M, Potter-Bynoe G, Roux D, Davis MR, Jr., et al. Parallel bacterial evolution within multiple patients identifies candidate pathogenicity genes. Nature genetics. 2011;43(12):1275-80.
32. Silva IN, Santos PM, Santos MR, Zlosnik JEA, Speert DP, Buskirk SW, et al. Long-term evolution of *Burkholderia multivorans* during a chronic cystic fibrosis infection reveals shifting forces of selection. mSystems. 2016;1(3):e00029-16.
33. Schaefers MM, Liao TL, Boisvert NM, Roux D, Yoder-Himes D, Priebe GP. An oxygen-sensing two-component system in the *Burkholderia cepacia* complex regulates biofilm, intracellular invasion, and pathogenicity. PLoS Pathog. 2017;13(1):e1006116.
34. Schaefers MM, Wang BX, Boisvert NM, Martini SJ, Bonney SL, Marshall CW, et al. Evolution towards Virulence in a *Burkholderia* Two-Component System. mBio. 2021;12(4):e01823-21.
35. Choi K-H, Mima T, Casart Y, Rholl D, Kumar A, Beacham IR, et al. Genetic tools for select-agent-compliant manipulation of *Burkholderia pseudomallei*. Applied and Environmental Microbiology. 2008;74(4):1064-75.
36. Choi KH, DeShazer D, Schweizer HP. mini-Tn7 insertion in bacteria with multiple *glmS*-linked *att*Tn7 sites: example *Burkholderia mallei* ATCC 23344. Nat Protoc. 2006;1(1):162-9.
37. Zhang JH, Chung TD, Oldenburg KR. A simple statistical parameter for use in evaluation and validation of high throughput screening assays. Journal of Biomolecular Screening. 1999;4(2):67-73.
38. Valvano MA. Intracellular survival of *Burkholderia cepacia* complex in phagocytic cells. Canadian Journal of Microbiology. 2015;61(9):607-15.
39. Schmerk CL, Valvano MA. *Burkholderia multivorans* survival and trafficking within macrophages. J Med Microbiol. 2013;62(Pt 2):173-84.
40. Mahenthiralingam E, Urban TA, Goldberg JB. The multifarious, multireplicon *Burkholderia cepacia* complex. Nat Rev Microbiol. 2005;3(2):144-56.
41. Kovacs-Simon A, Hemsley CM, Scott AE, Prior JL, Titball RW. *Burkholderia thailandensis* strain E555 is a surrogate for the investigation of *Burkholderia pseudomallei* replication and survival in macrophages. BMC microbiology. 2019;19(1):97.
42. Ravindranath PA, Forli S, Goodsell DS, Olson AJ, Sanner MF. AutoDockFR: Advances in Protein-Ligand Docking with Explicitly Specified Binding Site Flexibility. PLOS Comput Biol. 2015;11(12):e1004586-e.

43. Dubey BN, Lori C, Ozaki S, Fucile G, Plaza-Menacho I, Jenal U, et al. Cyclic di-GMP mediates a histidine kinase/phosphatase switch by noncovalent domain cross-linking. Sci Adv. 2016;2(9):e1600823.
44. Cai Y, Su M, Ahmad A, Hu X, Sang J, Kong L, et al. Conformational dynamics of the essential sensor histidine kinase WalK. Acta Crystallogr D Struct Biol. 2017;73(Pt 10):793-803.
45. Mideros-Mora C, Miguel-Romero L, Felipe-Ruiz A, Casino P, Marina A. Revisiting the pH-gated conformational switch on the activities of HisKA-family histidine kinases. Nature Communications. 2020;11(1):769.
46. Honorato RV, Koukos PI, Jimenez-Garcia B, Tsaregorodtsev A, Verlato M, Giachetti A, et al. Structural Biology in the Clouds: The WeNMR-EOSC Ecosystem. Front Mol Biosci. 2021;8:729513.
47. van Zundert GCP, Rodrigues JPGLM, Trellet M, Schmitz C, Kastritis PL, Karaca E, et al. The HADDOCK2.2 Web Server: User-Friendly Integrative Modeling of Biomolecular Complexes. Journal of Molecular Biology. 2016;428(4):720-5.
48. Nakamura H, Kumita H, Imai K, Iizuka T, Shiro Y. ADP reduces the oxygen-binding affinity of a sensory histidine kinase, FixL: the possibility of an enhanced reciprocating kinase reaction. Proc Natl Acad Sci USA. 2004;101(9):2742-6.
49. Gilles-Gonzalez MA, Ditta GS, Helinski DR. A haemoprotein with kinase activity encoded by the oxygen sensor of *Rhizobium meliloti*. Nature. 1991;350(6314):170-2.
50. Tay S, Yew W. Development of quorum-based anti-virulence therapeutics targeting Gram-negative bacterial pathogens. International Journal of Molecular Sciences. 2013;14(8):16570-99.
51. Gotoh Y, Eguchi Y, Watanabe T, Okamoto S, Doi A, Utsumi R. Two-component signal transduction as potential drug targets in pathogenic bacteria. Current Opinion in Microbiology. 2010;13(2):232-9.
52. Rasko DA, Moreira CG, Li de R, Reading NC, Ritchie JM, Waldor MK, et al. Targeting QseC signaling and virulence for antibiotic development. Science. 2008;321(5892):1078-80.
53. Barrett JF, Hoch JA. Two-component signal transduction as a target for microbial anti-infective therapy. Antimicrobial Agents and Chemotherapy. 1998;42(7):1529-36.
54. Johnson BK, Abramovitch RB. Small Molecules That Sabotage Bacterial Virulence. Trends Pharmacol Sci. 2017;38(4):339-62.
55. Johnson BK, Colvin CJ, Needle DB, Mba Medie F, Champion PA, Abramovitch RB. The Carbonic Anhydrase Inhibitor Ethoxzolamide Inhibits the *Mycobacterium tuberculosis* PhoPR Regulon and Esx-1 Secretion and Attenuates Virulence. Antimicrob Agents Chemother. 2015;59(8):4436-45.
56. Zheng H, Colvin CJ, Johnson BK, Kirchhoff PD, Wilson M, Jorgensen-Muga K, et al. Inhibitors of *Mycobacterium tuberculosis* DosRST signaling and persistence. Nature chemical biology. 2017;13(2):218-25.
57. Zheng H, Williams JT, Aleiwi B, Ellsworth E, Abramovitch RB. Inhibiting *Mycobacterium tuberculosis* DosRST Signaling by Targeting Response Regulator DNA Binding and Sensor Kinase Heme. ACS chemical biology. 2020;15(1):52-62.
58. Prieto JM, Rapún-Araiz B, Gil C, Penadés JR, Lasa I, Latasa C. Inhibiting the two-component system GraXRS with verteporfin to combat *Staphylococcus aureus* infections. Sci Rep. 2020;10(1):17939.
59. Kwiecinski JM, Jelani DA, Fuentes EJ, Horswill AR. Therapeutic Inhibition of *Staphylococcus aureus* ArlRS Two-Component Regulatory System Blocks Virulence. Antimicrob Agents Chemother. 2022;66(7):e0018722.
60. Allen RC, Popat R, Diggle SP, Brown SP. Targeting virulence: can we make evolution-proof drugs? Nat Rev Microbiol. 2014;12(4):300-8.
61. Choi KH, Schweizer HP. mini-Tn7 insertion in bacteria with single *att*Tn7 sites: example *Pseudomonas aeruginosa*. Nat Protoc. 2006;1(1):153-61.

609 62. Pettersen EF, Goddard TD, Huang CC, Couch GS, Greenblatt DM, Meng EC, et al.
610 UCSF Chimera--a visualization system for exploratory research and analysis. J Comput Chem.
611 2004;25(13):1605-12.
612 63. Laskowski RA, Swindells MB. LigPlot+: Multiple Ligand–Protein Interaction Diagrams for
613 Drug Discovery. Journal of Chemical Information and Modeling. 2011;51(10):2778-86.
614